

# Monocrystalline and Polycrystalline ZnO and ZnMnO Films Grown by Atomic Layer Epitaxy — Growth and Characterization

A. WÓJCIK<sup>a</sup>, K. KOPALKO<sup>b</sup>, M. GODLEWSKI<sup>a,b,\*</sup>,  
E. ŁUSAKOWSKA<sup>b</sup>, W. PASZKOWICZ<sup>b</sup>, K. DYBKO<sup>b</sup>,  
J. DOMAGAŁA<sup>b</sup>, A. SZCZERBAKOW<sup>b</sup> AND E. KAMIŃSKA<sup>c</sup>

<sup>a</sup>Dep. of Mathematics and Natural Sciences, College of Science  
Cardinal S. Wyszyński University, Warsaw, Poland

<sup>b</sup>Institute of Physics, Polish Academy of Sciences  
al. Lotników 32/46, 02-668 Warsaw, Poland

<sup>c</sup>Institute of Electron Technology, al. Lotników 32/46, 02-668 Warsaw, Poland

Recently we demonstrated growth of monocrystalline ZnO films by atomic layer epitaxy in the gas flow variant using inorganic precursors. In this study, we discuss properties of ZnO films grown with organic precursors. Successful Mn doping of the ZnO films during the growth was achieved using the Mn-thd complex. Secondary ion mass spectroscopy and X-ray investigations reveal the contents of Mn up to about 20% of the cationic component.

PACS numbers: 68.55.Jk, 68.55.Ln, 68.55.Nq, 78.66.Hf, 81.15.Kk

## 1. Introduction

ZnO films are intensively studied due to their potential applications in optoelectronics (UV light sources), gas sensors, piezoelectric sensors, transparent electrodes, as well as to their attractive magnetic properties created by doping with transition metal ions. Several alternative methods are applied to obtain ZnO films. This includes ion sputtering [1], reactive thermal evaporation [2], spray pyrolysis

---

\*corresponding author; e-mail: godlew@ifpan.edu.pl

[3], pulsed laser deposition [4], metal organic chemical vapor deposition (MOCVD) [5] and molecular beam epitaxy (MBE) [6,7].

Recently we reported successful growth of polycrystalline and crystalline ZnO films by atomic layer epitaxy (ALE) often referred to as atomic layer deposition (ALD) [8, 9]. In the recent years, the number of ALE(D) papers increases exponentially. At present the ratio of reports on ALD-grown materials versus MBE-grown approaches 1:4 and increases fast. This relates to simplicity and versatility of the ALE(D) method in which the reaction precursors are alternately introduced to the growth chamber. This enables one to use a wide range of precursor pairs of very different reactivity, including very reactive ones (not suitable for the CVD or MOCVD growth processes [10]). This quality of ALE(D) was utilized by us in the present study on growing ZnO films from a range of different inorganic (discussed elsewhere) and organic precursors. The growth details are given below.

## 2. ALE growth of ZnO films

Recently, we reported successful growth of ZnO films using simple inorganic zinc precursors, such as metal Zn or  $\text{ZnCl}_2$ . Monocrystalline ZnO films were obtained only on GaN/sapphire substrates [9]. Films grown on soda lime glass, sapphire, or silicon ((001) or (111)) were polycrystalline [8]. The use of simple inorganic precursors resulted however in relatively low growth rates. Films of a thickness of few hundred nm were typically obtained in the ALE process consisting of 4000 cycles.

We tested several organic zinc precursors to increase the growth rates. In this work, we discuss properties of the ZnO films obtained using zinc acetate ( $\text{Zn}(\text{CH}_3\text{COO})_2$ ) as organic zinc precursor. We report also on two new ALE(D) processes performed to optimize Mn doping of our films.

### 2.1. ZnO films grown from zinc acetate

ZnO films were obtained by hydrolysis of zinc acetate (see Ref. [10] and references given in). Growth was performed at 360°C substrate (sapphire) temperature, temperature of zinc source of 250°C with 0.5 to 1 s long ALE(D) pulses. Nitrogen gas was used as transport and valving gas. Processes performed at lower substrate temperature resulted in polycrystalline films of lower quality with grains of a smaller size. Use of zinc organic precursor (water was used as oxygen source) resulted in larger growth rates. Films of micrometer thickness were obtained in our typical ALE(D) processes of 4000 cycles.

### 2.2. Mn doping of ZnO films

Mn doping with inorganic precursors (metal Mn,  $\text{MnCl}_2$ ,  $\text{MnI}_2$ ) resulted in relatively low Mn concentrations in the films, well below 1%. This is why we turned our attention to more reactive organic Mn precursors. Two types of such precursors

were tested in the present work. We used either Mn-thd (2, 2, 6, 6-tetramethyl-3, 5-heptanedione) or Mn-acac ( $C_{15}H_{21}MnO_6$ ) as organic Mn sources. Properties of these precursors are discussed in [10]. These precursors enabled us to obtain significantly larger Mn fractions in ZnO, reaching, in the case of Mn-thd precursors, up to about 20%, as concluded from secondary ion mass spectroscopy (SIMS) measurements. Mn precursors were kept at 160°C temperature, whereas other growth parameters were maintained, as in the process described above.

We tested two growth methods to introduce Mn into ZnO lattice. In the first one we first grew ZnO layer using zinc acetate and water vapor and a glass or sapphire substrate kept at 360°C. Then ZnO film was covered with MnO layer in the process performed at reduced temperature of 200°C, using Mn-thd precursor and water vapor. This process led to the highest Mn fraction in our films (about 20%, as concluded from SIMS measurements). Most surprisingly Mn fraction in a film was fairly in-depth homogeneous, as concluded from the SIMS investigations, indicating Mn–Zn intermixing during the MnO growth. In the second process we sequentially introduced to the growth chamber either zinc precursor or Mn organic precursor together with water vapor as oxygen source. This process resulted in lower Mn fractions in our films, but in our opinion decreased the chance of  $MnO_x$  precipitates.

Below we shortly discuss structural, optical, and electrical properties of the ZnO and ZnMnO films grown using organic precursors.

### 3. Characterization of ZnO and ZnMnO films

As already mentioned, the use of organic zinc precursors resulted in significantly increased growth rates. Film thicknesses up to 4 micrometers were achieved, which indicated growth rates increased by the factor of 8, as compared to processes with inorganic zinc precursors. These films show however worse surface morphology, as demonstrated in Fig. 1, comparing atomic force microscopy (AFM) images taken for two types of ZnO films: (a) for monocrystalline film grown on GaN/sapphire with inorganic zinc precursor and (b) for ZnO/sapphire film grown using zinc acetate. Granular microstructure of the latter film was observed, with relatively large height fluctuations of about 12.5 nm. This value was observed for as-grown films without any post-growth heat treatment.

Optical properties of the films depended on the post-growth annealing in oxygen. Before annealing only deep levels related photoluminescence (PL) bands were observed, whereas annealing results in appearance of sharp exciton-related bands in the band-edge region of the PL spectrum, indicating good quality of our ZnO films.

X-ray diffraction investigations (Fig. 2) indicate different growth mechanism for films grown with zinc acetate. Surprisingly, these films grow with the *c*-axis in the film plane, instead of usually observed *c*-axis being perpendicular to the

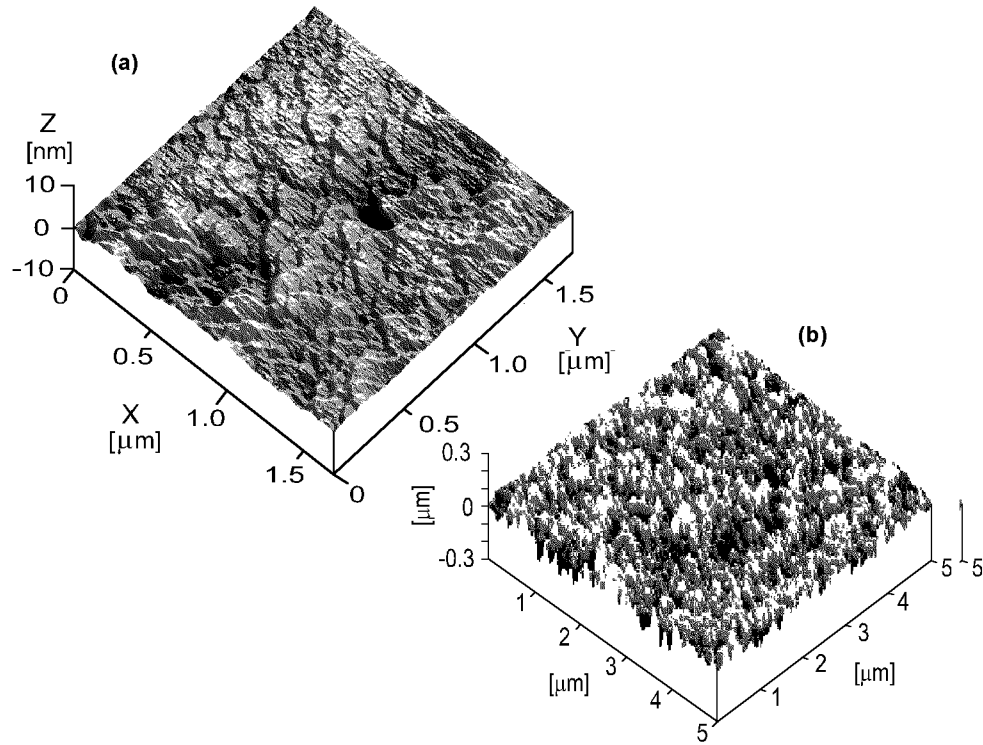


Fig. 1. AFM images for (a) ZnO/GaN/sapphire monocrystalline film grown using inorganic precursors (properties of these films are discussed in [9]) and (b) of ZnO/sapphire film grown using zinc acetate as zinc precursor. Different scales are used for  $x$ ,  $y$ , and  $z$  axes in the AFM images following considerable differences in the film roughness.

surface. Even more surprisingly, this growth mode changes upon doping. For Mn doped layers growth with the  $c$ -axis normal to the film surface is observed once more (Fig. 2).

Mn presence in our ZnO films was confirmed by SIMS, X-ray (energy dispersive X-ray fluorescence (EDXRF)), and optical investigations. The highest Mn fraction obtained by us was about 20%, as indicated by SIMS analysis. As mentioned above, this Mn fraction was achieved in the process in which MnO layer was grown on top of ZnO. Despite the fact that SIMS indicated very homogeneous in-depth Mn concentration of such films (doped using the Mn-thd precursor), we tested later on process in which Mn precursor was introduced every third cation precursor pulse.

We first compared efficiency of doping using two organic Mn precursors, while keeping the similar ALE(D) sequences. The Mn-acac precursor proved to be less efficient than Mn-thd one, resulting in slightly smaller Mn fractions (see Fig. 3).

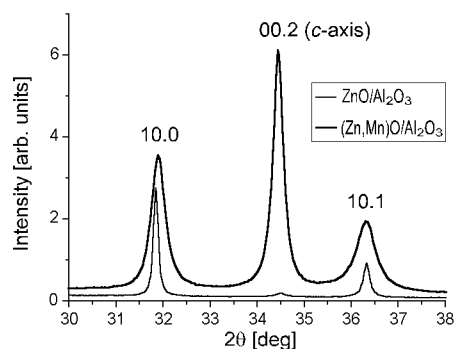


Fig. 2. X-ray diffraction patterns showing two different growth modes for ZnO undoped and doped Mn using organic precursors. For Mn doped layers strong  $c$ -axis related reflection is observed indicating growth mode with  $c$ -axis normal to the film plane.

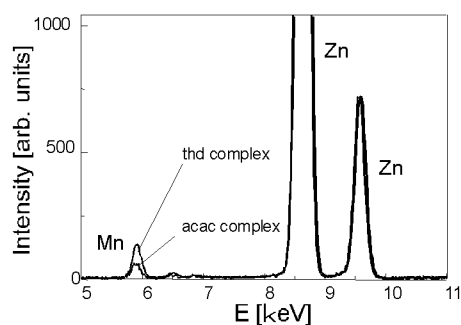


Fig. 3. Comparison of EDXRF spectra taken for ZnMnO films grown by ALE(D) using two types of organic Mn precursors, as indicated in the figure.

It is fairly difficult to estimate exact Mn fraction in our films. SIMS and X-ray investigations, including micro-probe study (EDXRF), confirm Mn presence in the layers, but leave an open question on rate of Mn substitution into the ZnO lattice. We believe that at least part of Mn is introduced into lattice sites replacing zinc. First of all, we observed that Mn doping causes a shift of the band gap of ZnO. The results of optical absorption experiments are shown in Fig. 4, demonstrating a noticeable shift of band gap as a result of Mn doping. It is however not known how the band gap of ZnO should change upon Mn doping, so we could not determine exact Mn fractions in our films from the observed shifts of fundamental band-gap energy. In turn, X-ray analysis indicated a change of lattice parameters upon Mn introduction. Rough estimation from these X-ray data (we estimated how the lattice parameter should change for ZnMnO films depending on Mn fraction) indicated 6 to 8% Mn fraction in ZnMnO layer studied in optical absorption experiment shown in Fig. 4. Exact Mn standards for SIMS and EDXRF experiments are required for detailed estimation of Mn fractions in our films.

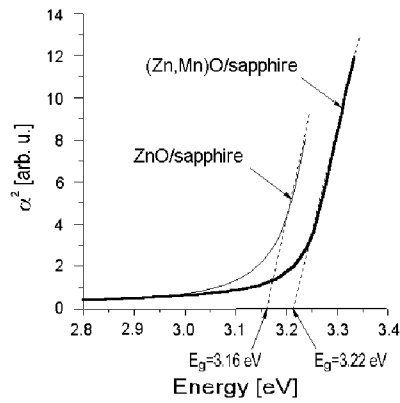


Fig. 4. Shift of a fundamental energy band gap when ZnO doped by Mn. Mn fraction in the film studied was about 6 to 8%, but exact value remains unknown.

Electrical measurements indicate preferential *n*-type conductivity of our films. Film conductivity depended on the growth details and on the film thickness. The highest conductivity was observed for thick films grown on sapphire using organic precursors, whereas the films grown on soda lime glass were resistive. Mn doping has rather small effect on the film resistivity.

#### 4. Conclusions

We report successful growth of ZnO films by atomic layer epitaxy. Crystallinity of ZnO films depended on the substrate and on precursors used in the process. Monocrystalline films were grown using inorganic precursors when lattice matched substrate was used. The use of organic precursors resulted, on one hand, in enhanced growth rate and better optical properties of the films, but, on other hand, in rougher film surfaces. The application of organic Mn precursors opens chance of growing diluted magnetic semiconductor samples with large Mn fractions. Films with Mn-fractions of up to 20% were obtained in the process in which ZnO film was first grown covered then with MnO film. Their magnetic properties are presently under investigations.

#### Acknowledgment

The authors thank Prof. L. Niinistö for valuable advices regarding the ALE growth method. This work was partly supported by grant no. PBZ-KBN-044/P03/2001 of the State Committee for Scientific Research. The ALE reactor was bought using SEZAM grant of Foundation for Polish Science.

## References

- [1] H. Nanto, T. Minami, S. Takata, *Phys. Status Solidi A* **65**, K131 (1981).
- [2] H. Morgan, D.E. Brodie, *Can. J. Phys.* **60**, 1387 (1982).
- [3] J. Aronovich, A. Ortiz, R.H. Bube, *J. Vac. Sci. Technol.* **16**, 994 (1979).
- [4] R.D. Vispute, V. Talyansky, S. Choopun, R.P. Sharma, T. Venkatesan, M. He, X. Tang, J.B. Halpern, M.G. Spencer, Y.X. Li, L.G. Salamanca-Riba, A.A. Iliadis, K.A. Jones, *Appl. Phys. Lett.* **73**, 348 (1998).
- [5] S. Bethke, H. Pan, B.W. Wesseis, *Appl. Phys. Lett.* **52**, 138 (1988).
- [6] Y. Chen, D.M. Bagnall, H.J. Koh, K.T. Park, K. Hiraga, Z. Zhu, T. Yao, *J. Appl. Phys.* **84**, 3912 (1998).
- [7] P. Zu, Z.K. Tang, G.K.L. Wong, M. Kawasaki, A. Ohtomo, H. Koinuma, Y. Seifawa, *Solid State Commun.* **103**, 459 (1997).
- [8] K. Kopalko, M. Godlewski, E. Guziewicz, E. Łusakowska, W. Paszkowicz, J. Domagała, E. Dynowska, A. Szczerbakow, A. Wójcik, M.R. Phillips, *Vacuum* **74**, 269 (2004).
- [9] K. Kopalko, M. Godlewski, J.Z. Domagała, E. Lusakowska, W. Paszkowicz, A. Szczerbakow, *Chem. Mater.* **16**, 1447 (2004).
- [10] L. Niinistö, J. Päiväsaari, J. Niinistö, M. Putkonen, M. Nieminen, *Phys. Status Solidi A* **201**, 1443 (2004).